Creation of ray modes by strong random scattering

K. Ziegler

Institut für Physik, Universität Augsburg
D-86135 Augsburg, Germany

In the presence of strong random scattering the behavior of particles with degenerate spectra is quite different from Anderson localization of particles in a single band: it creates geometric states rather than confining the particles to an area of the size of the localization length. These states are subject to a Fokker-Planck dynamics with universal drift velocity and disorder dependent diffusion coefficient. This behavior has some similarity with the unidirectionally propagating edge states in quantum Hall systems.

Random scattering of wave-like states (electrons, photons or acoustic waves) leads either to diffusion for weak random scattering or to Anderson localization (AL) in the presence of strong random scattering. AL is a phenomenon where diffusion or propagation is suppressed because random scattering confines the modes to a finite region, whose size is characterized by the localization length [1–3]. The characteristics of AL can be observed in a pure form for photons [4–6] due to the absence of an additional particle-particle interaction.

Another interesting phenomenon in disordered systems is the quantum Hall effect, which is characterized by plateaux in the Hall conductivity [7]. The latter have been attributed to propagating edge modes in the otherwise Anderson localized bulk system [8]. Edge modes also exist in gapped systems without any random scattering. A simple case is a massive 2D Dirac Hamiltonian, whose mass sign changes by crossing an edge in y-direction: The mass is $-m$ for $x < 0$ and m for $x > 0$. The gap $2|m| > 0$ prevents the system to generate any other extended state than that along the edge. This mode decays exponentially when we go away from the edge in x-direction. The appearence of such states can be realized in a photonic crystal with Faraday effect [9].

It was recently observed that similar one-dimensional modes can also be generated spontaneously by strong scattering in 2D systems without the existence of any edge [10, 11]. These states, which will be called ray modes subsequently, are created in systems with a generalized particle-hole symmetry. The latter implies spectral degeneracies [11]. This is caused by the fact that the Hamiltonian H acts on states Ψ_{rj} that depend on space coordinates r and on an additional spinor index j, typically with values $j = 1, 2$. Then there exists a unitary matrix U that acts only on the spinor index and which transforms H into $-H^*$ as

$$H = -UH^*U^\dagger . \qquad (1)$$

In this paper we will show that ray modes can be created spontaneously by strong random scattering in systems with spectral degeneracies based on the relation (1). Starting point is the transition probability for a particle, governed by the random Hamiltonian H, to move from the site r' on a lattice to another lattice site r within the time τ:

$$P_{rr'}(\tau) = \sum_{j,j'} \langle |\langle r, j|e^{-iH\tau}|r', j'\rangle|^2 \rangle_d , \qquad (2)$$

where $\langle r, j|...|r', j'\rangle$ is the quantum average and $\langle ... \rangle_d$ is the average with respect to randomly distributed disorder. r and r' refer to real space coordinates and the indices j, j' refer to different bands of the system. $P_{rr'}(\tau)$ is a fundamental quantity from which we can obtain transport and localization properties [12, 13].

In the following we will focus on 2D Dirac and 3D Weyl particles and on particles on the square lattice with π flux. For all these models the Hamiltonian reads in sublattice representation

$$H = \vec{\sigma} \cdot \vec{H} + \sigma_0 V , \qquad (3)$$

where σ_j ($j = 0, 1, 2, 3$) are Pauli matrices with the 2×2 unit matrix σ_0 and a random potential V with mean zero and variance $\langle V_r V_{r'}\rangle_d = g\delta_{rr'}$. The part with σ_1, σ_2 provides scattering between different values of j, which will be crucial for the subsequent discussion.

The relation (1) is satisfied, for instance, for the block-diagonal matrix of the 3D gapless Weyl Hamiltonian $diag(\sigma_1 p_1 + \sigma_2 p_2 + \sigma_3 p_3 + V\sigma_0, \sigma_1 p_1 + \sigma_2 p_2 - \sigma_3 p_3 - V\sigma_0)$ with

$$U = \frac{1}{\sqrt{2}} \begin{pmatrix} 0 & \sigma_1 \\ \sigma_1 & 0 \end{pmatrix} , \qquad (4)$$

where p_j is the momentum operator with $p_j^* = -p_j$. Another example is the massive 2D Dirac Hamiltonian $diag(\sigma_1 p_1 + \sigma_2 p_2 + \sigma_3 m + V\sigma_0, \sigma_1 p_1 + \sigma_2 p_2 + \sigma_3 m - V\sigma_0)$, which also obeys condition (1).

It was shown in Ref. [10] that the Fourier component $\tilde{P}_{rr'}(i\epsilon)$ of $P_{rr'}(\tau)$ agrees for large distances $|r - r'|$ with a correlation function of a random-phase model, defined by the random matrix

$$C_{rr'} = 2\delta_{rr'} - \sum_{j,j'} h_{rj,r'j'} \sum_{j'',r''} h_{r'j',r''j''}^{\dagger} , \quad (5)$$

where the propagator

$$h_{rr'} = \sigma_0 \delta_{rr'} + 2i\eta(\mathcal{H} - i\bar{\eta}\sigma_0)_{rr'}^{-1} \quad (6)$$

depends on the random phase Hamiltonian

$$\mathcal{H}_{rj,r'j'} = e^{i\alpha_{rj}} \bar{H}_{rj,r'j'} e^{-i\alpha_{r'j'}} . \quad (7)$$

$\bar{H} = \langle H \rangle_d$ is the average Hamiltonian and η is the scattering rate while $\bar{\eta} = \eta + \epsilon$. η can be considered as an empirical parameter or can be calculated self-consistently from the self-energy of the average one-particle Green's function $\langle (H - z)^{-1} \rangle_d$ [14]. In any case, it increases with variance g of the random potential.

In the limit $\epsilon \to 0$ the propagator h is unitary since

$$hh^{\dagger} = \mathbf{1} - 4\epsilon\eta(\mathcal{H}^2 + \bar{\eta}^2\sigma_0)^{-1} . \quad (8)$$

Then there is the following asymptotic relation for large scales between the random phase model and the Fourier components of the average transition probability [10]:

$$\tilde{P}_{rr'}(i\epsilon) \sim \frac{\langle C_{rr'}^{-1} \det C \rangle_a}{\langle \det C \rangle_a} , \quad (9)$$

where the brackets $\langle ... \rangle_a$ mean integration with respect to the angular variables $\{0 \le \alpha_{rj} < 2\pi\}$, normalized by 2π. These random angles represent the relevant part of the disorder fluctuations in terms of long-range correlations. In other words, there is a mapping from the original random Hamiltonian in Eq. (3) to the random phase Hamiltonian $\mathcal{H}$ that preserves the long-range correlations.

The expression (9) can be calculated for strong scattering in powers of the expansion parameter E_b/η (E_b: bandwidth), combined with a mean-field approximation as the starting point for the expansion. It has to be chosen such that the expansion is convergent.

Mean-field approximation: The (unnormalized) distribution density $\det C$ in Eq. (9) is approximated by a constant phase $\alpha_{rj} \approx \bar{\alpha}_j$ and the exact value is approached systematically by a convergent expansion in terms of the phase factor fluctuations $e^{\alpha_{rj}} - e^{\bar{\alpha}_j}$. First, it should be noticed that

there is an invariance of C with respect to a global phase change $\alpha_{rj} \to \alpha_{rj} + \phi$. This implies that the mean-field distribution depends only on the relative phase difference $\Delta = \bar{\alpha}_1 - \bar{\alpha}_2$. Its value is determined by the condition $\max_\Delta \int_p \log(|\tilde{C}_p(\Delta)|)$, where $\tilde{C}_p(\Delta)$ are the Fourier components of C with uniform phases. This condition may have several solutions Δ_l with the same maximum, such that we have to sum over all of them:

$$\det C \approx \sum_l \exp\left[\int_p \log(\tilde{C}_p(\Delta_l))\right] . \quad (10)$$

It turns out that the Fourier components $\tilde{C}_p(\Delta_l)$ can be written as

$$\tilde{C}_p(\Delta) = 2 - \pi_0 - \vec{s} \cdot \vec{\pi} \quad (11)$$

with $\pi_j = Tr_2(\sigma_j \bar{h}_p \bar{h}_{p=0}^{\dagger})$ for $j = 0, 1, 2$,

$$\bar{h}_p = \sigma_0 + 2i\eta(\bar{H}_p - i\bar{\eta}\sigma_0)^{-1} , \quad (12)$$

and with the 2D unit vector $\vec{s} = (\cos\Delta, \sin\Delta)$. Then Eq. (9) reads in this mean-field approximation

$$\tilde{P}_{rr'}(i\epsilon) \approx 2 \int_p e^{-ip \cdot (r-r')} \sum_l \frac{1}{\tilde{C}_p(\Delta_l)} . \quad (13)$$

The pole of $1/\tilde{C}_p(\Delta_l)$ with respect to ϵ gives, after the analytic continuation $\epsilon \to i\omega$, the effective dispersion ω_p of the new mode. This pole depends strongly on the details of the Hamiltonian components with Pauli matrices σ_1 and σ_2. It is important that we are only interested in the long range regime of $\tilde{P}_{rr'}(i\epsilon)$; i.e., in the behavior for small momenta. Therefore, we focus on $\bar{h}_p$ for small p, and according to the expressions in (11) and (12), this means that we need $\vec{s} \cdot \vec{H}_p$ for small p. In the following we calculate (11) for three different models, namely 2D massive Dirac particles, 3D Weyl particles and particles on a square lattice with π flux, whose low energy Hamiltonians behave like $H \sim \vec{\sigma} \cdot \vec{p}$ for small p.

2D Dirac particles: For massive 2D Dirac fermions on a torus the Hamiltonian reads $\tilde{H}_p = \vec{\sigma} \cdot \vec{p} + \sigma_3 m$ ($0 \le p_j < 2\pi$). Then we obtain

$$\tilde{h}_p = \sigma_0 + \frac{2i\eta}{p^2 + m^2 + \bar{\eta}^2} (\vec{\sigma} \cdot \vec{p} + \sigma_3 m + i\sigma_0 \bar{\eta})$$

and $\vec{s} = (\cos(\Delta + \theta), \sin(\Delta + \theta))$ for $\tilde{C}_p(\Delta)$, which depends on the angle $\theta = \arctan(2m\eta/(m^2 - \bar{\eta}^2))$. For $\epsilon \sim 0$ we obtain

$$\frac{1}{\tilde{C}_p(\Delta)} \sim \frac{(p^2 + m^2 + \bar{\eta}^2)/2\eta}{2\epsilon + i\vec{s} \cdot \vec{p} + \bar{\eta}p^2/(m^2 + \bar{\eta}^2)} , \quad (14)$$
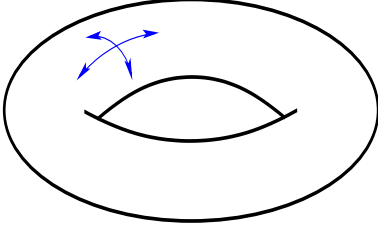
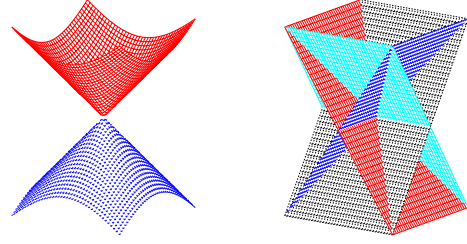FIG. 1: Four ray modes on a torus, created by strong random scattering.

FIG. 2: Linear Dirac dispersion (left) and the linear dispersion of the four ray modes (right). The latter consists of four intersecting planes whose slopes agree up to a factor 1/2 with those of the Dirac dispersion.

whose pole give the dispersion of a ray mode

$$\omega_p \sim \frac{1}{2}\vec{s}\cdot\vec{p} - iDp^2 \quad \text{with} \quad D = \frac{\eta}{2(m^2+\eta^2)} \; . \quad (15)$$

The second term of ω_p is imaginary and describes damping. The mean-field condition $\max_\Delta \int_p \log(|\tilde{C}_p(\Delta)|)$ is solved by $\Delta + \theta = 0, \pi/2, \pi, 3\pi/2$. Thus, four rays are created by strong random scattering with unit vectors $\vec{s}_{1,3} = (\pm 1, 0)$ and $\vec{s}_{2,4} = (0, \pm 1)$ (cf. Fig. 1). The linear dispersion without damping is shown on the right-hand side of Fig. 2.

The dispersion (15) can also be understood as a Fokker-Planck dynamics with drift velocity $\vec{s}$ [15]. This can be seen when we calculate the transition probability from the expression (14) within a Fourier representation in time and space. By assuming that the propagation starts from the initial site 0 we get for the transition probability in Eq. (2) for each of the four ray modes

$$P_{\vec{r}}(\tau) \sim \frac{1}{\tau D 4\pi} \exp\left[-\frac{1}{4D\tau}(\vec{r}+\tau\vec{s}_l)^2\right] \quad (16)$$

with the effective diffusion coefficient D, which is the damping coefficient in Eq. (15). This result describes diffusion with a propagating (drifting) center in the direction of $\vec{s}_l$. The damping term in the dispersion (15) leads to an additional diffusion away from these propagating centers. Diffusion slows down as the scattering rate η is increased. This indicates that strong random scattering confines (or localizes) the movement of the particle to rays along the unit vectors $\vec{s}_l$.

3D Weyl particles: The Hamiltonian for 3D Weyl particles with 3D momentum $\vec{p}$ reads $\tilde{H}_p = \vec{p}\cdot\vec{\sigma}$. This implies for the propagator

$$\tilde{h}_p = \sigma_0 + \frac{2i\eta}{p^2+\bar{\eta}^2}(\vec{\sigma}\cdot\vec{p} + i\sigma_0\bar{\eta})$$

from which we obtain

$$\frac{1}{\tilde{C}_p(\Delta)} \sim \frac{(p^2+\bar{\eta}^2)/2\bar{\eta}}{2\epsilon + i\vec{s}\cdot\vec{p} + p^2/\bar{\eta}} \; .$$

Then the dispersion of the ray modes reads

$$\omega_p \sim \frac{1}{2}\vec{s}\cdot\vec{p} - iDp^2 \; . \quad (17)$$

Since the mass is zero in this case, the damping coefficient is $D = 1/2\eta$. Although the Hamiltonian is isotropic in 3D, there are again only four ray modes on the x-y torus.

Square lattice with π flux: The square lattice is bipartite. Therefore, the tight-binding Hamiltonian for particles on a square lattice, which describes nearest-neighbor hopping matrix elements, can be written in terms of two sublattices with coordinates (rj) ($j = 1, 2$ and r are the coordinates on the sublattice with $j = 1$). Including the Peierls phase factors for the π flux with $\pm i$ in x-direction and ± 1 in y-direction, as indicated in Fig. 3, the corresponding Hamiltonian reads

$$\tilde{H}_p = \vec{\sigma}\cdot\vec{P} + \sigma_3 m, \quad P_j = t\sin ak_j \; . \quad (18)$$

This is a discretized 2D Dirac Hamiltonian with a lattice constant a and the hopping energy t. The flux through a plaquette of the square lattice is -1, which is related to a phase π. There is also a term with mass m that represents a staggered potential with m ($-m$) on sublattice $j = 1$ (sublattice $j = 2$). This Hamiltonian also obeys property (1) as described for the 2D Dirac Hamiltonian. The form of this Hamiltonian allows us to apply directly the results of the 2D Dirac Hamiltonian that gives

$$\frac{1}{\tilde{C}_p(\Delta)} \sim \frac{(P^2+m^2+\bar{\eta}^2)/2\eta}{2\epsilon + i\vec{s}\cdot\vec{P} + \bar{\eta}P^2/(m^2+\bar{\eta}^2)} \; .$$

This implies the dispersion

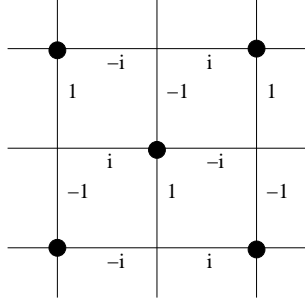$$\omega_p \sim \frac{1}{2}\vec{s}\cdot\vec{P} - iDP^2 \quad (19)$$

FIG. 3: Square lattice with π flux as defined by the tight-binding Hamiltonian (18). The dots represent the sublattice with index $j = 1$ and the complex numbers are the Peierls phase factors for hopping from $j = 1$ to $j = 2$.

for the ray mode on a square lattice with π flux with the same directions as in the two previous cases. Here it should be noticed that there are small values for P_j near the four spectral nodes with $ak_j = 0, \pm\pi$.

Discussion: The effect of strong random scattering in models with a Weyl-Dirac Hamiltonian and for the tight-binding Hamiltonian on the square lattice with π flux does not lead to conventional AL but creates four orthogonal ray modes. For periodic boundary conditions the ray modes are parallel to a torus or follow its circumference (cf. Fig. 1). The spontaneous creation of the four ray modes can be understood as an azimuthal localization at four discrete angles. In contrast to isotropic diffusion or isotropic Anderson localization, the states are confined to four orthogonal directions. This is similar to the uni-directional edge states in the quantum Hall effect or in photonic crystals with Faraday effect [9]. The mechanisms for their creation are rather different, though. Whereas the edge states are created in gapped photonic crystals at interfaces between regions with different Chern numbers [9], strong randomness creates the ray modes spontaneously in an isotropic system with strong random scattering. This makes them more accessible in real materials, provided that a band structure with linear dispersion exists for in-

terband scattering.

The result of the calculation can be summarized as a mapping of the momentum part of the Dirac-Weyl Hamiltonian to the ray-mode dispersion as

$$\vec{\sigma} \cdot \vec{p} \;\; \rightarrow \;\; \frac{1}{2}\vec{s} \cdot \vec{p} - iDp^2 \; . \qquad (20)$$

Thus, in all three cases we have considered here, the Pauli matrix vector $\vec{\sigma}$ is replaced by the vector $(1/2)\vec{s}$, whose components are scalars. Moreover, there is an additional damping term, whose coefficient D in Eq. (15) decreases with an increasing scattering rate and increasing gap. The mapping (20) is reminiscent of the renormalization of the average one-particles Green's function as found, for instance, in the form of a complex self-energy in the self-consistent Born approximation. In the case of 2D Weyl particles we get from random scattering the mapping

$$\vec{\sigma} \cdot \vec{p} \;\; \rightarrow \;\; \vec{\sigma} \cdot \vec{p} + i\sigma_0\eta \; .$$

In contrast to the constant scattering rate η, the damping of the ray modes vanishes quadratically for small momenta.

The fact that, for instance, photons can escape from a cloud of random scatterers is similar to the phenomenon of Klein tunnelling in a system with a potential barrier [16, 17]. As in the latter case, it is crucial that there are two spectral bands. In our calculation this is reflected by the term $\vec{s}\cdot\vec{\pi}$ in (11). It is sufficient for the generation of ray modes that this term vanishes linearly with the momentum.

Tight-binding models on the square or the honeycomb lattice without flux do not develop ray modes because $\vec{s} \cdot \vec{\pi}$ (or equivalently $\vec{s} \cdot \vec{H}$) is not linear for small momenta, as a calculation of the inverse propagator (11) indicates. However, the linear behavior of $\vec{s} \cdot \vec{H}$ at small momenta might be obtained by breaking the time-reversal invariance: either by a periodic magnetic flux [18], by an additional spin texture on the honeycomb lattice [19], or by the Faraday effect of a magneto-optic medium in a photonic crystal [9].

[1] P.W. Anderson, Phys. Rev. **109**, 1492 (1958).
[2] E. Abrahams, P.W. Anderson, D.C. Licciardello and T.V. Ramakrishnan, Phys. Rev. Lett. **42**, 673 (1979).
[3] F. Wegner, Z. Phys. B **35**, 207 (1979).
[4] J.M. Drake and A.Z. Genack, Phys. Rev. Lett. **63**, 259 (1989).
[5] D.S. Wiersma, P. Bartolini, A. Lagendijk, and R. Righini, Nature **390**, 671 (1997).
[6] T. Sperling, W. Bührer, C.M. Aegerter and G. Maret, Nature Photonics **7**, 48 (2013).
[7] K. von Klitzing, G. Dorda, and M. Pepper, Phys. Rev. Lett. **45**, 494 (1980).
[8] R.E. Prange and S.M. Girvin, *The Quantum Hall*

Effect, Springer-Verlag (1987).

[9] S. Raghu and F.D.M. Haldane, Phys. Rev. A **78**, 033834 (2008).

[10] K. Ziegler, J. Phys. A: Math. Theor. **48**, 055102 (2015).

[11] K. Ziegler, arXiv:1412.7732

[12] D.J. Thouless, Phys. Rep. **13**, 93 (1974).

[13] A.J. McKane and M. Stone, Annals of Physics **131**, 36 (1981).

[14] J.W. Negele and H. Orland, *Quantum Many-particle Systems*, Westview Press, (2008).

[15] H. Risken, *The Fokker–Planck Equation: Methods of Solutions and Applications*, 2nd edition, Springer (1996); C.W. Gardiner, *Stochastic Methods*, 4th edition, Springer (2009).

[16] O. Klein, Z. Phys. **53**, 157 (1929).

[17] M.I. Katsnelson, K.S. Novoselov & A.K. Geim, Nature Physics **2**, 620 (2006).

[18] F.D.M. Haldane, Phys. Rev. Lett. (1988).

[19] A. Hill, A. Sinner and K. Ziegler, New J. Phys. **13**, 035023 (2011).